ORIGINAL ARTICLE

Changes in characteristics of climate extremes from 1961 to 2017 in Qilian Mountain area, northwestern China

LingLing Song[1] · Qing Tian[1] · ZongJie Li[2] · Yue Ming Lv[3] · Juan Gui[3] · BaiJuan Zhang[3] · Qiao Cui[3]

Abstract

In this study, the temporal and spatial characteristics of extreme climate from 1961 to 2017 were analyzed using daily precipitation and temperature data from 24 meteorological stations in the Qilian Mountain area, northwestern China. The results showed that warming accelerated considerably after 1985, particularly during the 1990s. The warming trend then increased after 2000 and further increased after 2010. The Qilian Mountains and the Hexi and Qaidam Inland River Basins greatly affected the Atlantic Multidecadal Oscillation (AMO), Northern Tropical Atlantic Index (NTA), Caribbean sea-level surface temperature (SST) Index (CAR), South China Sea Summer Monsoon Index (SCSSMI), and South American Summer Monsoon Index (SAMSMI). The circulation index on the extreme temperature warm index was stronger than that of the extreme temperature cold index. There were greater increases in all extreme indexes in the central part of the Qilian Mountain area, and the region of increase decreased from inside to outside. The interannual change in the warming index of extreme temperature was similar to that of the cold index of extreme temperature. TX10, TN10, ice days (ID), and frost days (FD) showed significant negative correlations with altitude, whereas TXN and TNN showed significant positive correlations with altitude. Changes in TX10, TN10, TXN, TNN, ID, FD, and diurnal temperature range were most noticeable in high-altitude areas (> 2500 m), whereas changes in TN90, TX90, TXX, TNX, and growing season length were most noticeable in low altitude areas (< 2500 m). The Qilian Mountain area and the Hexi and Qaidam Inland River Basins were greatly affected by the AMO, NTA, CAR, SCSSMI, and SAMSMI; however, they were only slightly affected by the Nino4, Northern Atlantic Oscillation, North Pacific model, Southern Oscillation Index, Arctic Oscillation, and Multiple ENSO Index. The effect of the circulation index of Atlantic Multidecadal Oscillation, Tropical Northern Atlantic Index, Tropical Southern Atlantic Index, North Tropical Atlantic SST Index, and CAR on the extreme temperature warm index was stronger than that of the extreme temperature cold index.

Keywords Climate change · Extreme temperature indexes · Extreme precipitation indexes · Qilian Mountain area

Introduction

The fifth Assessment Report of the Intergovernmental Panel on Climate Change (IPCC 2013) showed that the atmospheric and oceanic system is warming at an unprecedented pace and that the cover of ice and snow is rapidly decreasing. Such changes have been contributing to rising sea levels and increased greenhouse gas emissions since the 1950s. China is experiencing a significant impact from global climate change, and the rate of heating has been significantly higher than that of the global average level within the same period. From 1951 to 2020, China's annual average surface temperature showed a significant upward trend, with a heating rate of 0.26 °C/10 a, and the past 20 years have been the warmest since the beginning of the twentieth century

✉ Qing Tian
  tqing@gsau.edu.cn

[1] College of Forestry, Gansu Agricultural University, Lanzhou 730070, Gansu, China

[2] College of Energy and Power Engineering, Lanzhou University of Technology, Lanzhou 730050, China

[3] Key Laboratory of Ecohydrology of Inland River Basin/Gansu Qilian Mountain Ecology Research Center, Northwest Institute of Eco-Environment and Resources, Chinese Academy of Sciences, Lanzhou 730000, China

(CMA Climate Change Centre 2021). Extreme low-temperature events have shown a decreasing trend due to global warming, but extreme high-temperature events have shown an increasing trend, and heat waves are occurring more frequently (Easterling et al. 2000; Roy 2019; Rashid et al. 2020; Sangkharat et al. 2020).

Extreme climate events have a significant negative impact on human lives and natural ecosystems, and they disrupt food production and water supplies, destroy infrastructure and settlements, and increase morbidity and mortality (Singh et al. 2019; Li et al. 2019). In recent years, many studies have investigated different types of extreme climate events on different scales. The general tendency of extreme temperatures in Australia, West Africa, Asia–Pacific, and Indo-Pacific regions has changed in correspondence with global extreme temperature changes, and extreme temperature changes in China are generally consistent with those of global change. Although regional characteristics differ, the extreme maximum temperature has increased in northern China over the past 50 years (He et al. 2018; Yin et al. 2020). Zhai et al. (2003) analyzed extreme minimum temperature. Studies have shown that the numbers of cold (warm) nights have significantly reduced (increased). In addition, cold days, cold nights, warm days, and warm nights have undergone warming trends in more than 70% of global areas (Alexander et al. 2006; Almazroui and Saeed 2020). Zhou et al. (2010) found a significant decreasing trend in the number of frost days and freezing days in mainland China, and the most significant reductions are concentrated in the northern part of China. In contrast, the number of summer days and hot nights has increased significantly.

Areas showing significant increases are mainly located in central and eastern regions. Studies have detected extreme precipitation events occurring on different scales, and there are likely to be significant increases in strong precipitation events in regions with increased total precipitation on a global scale. It has been shown that even if the average amount of total precipitation decreases or remains unchanged, the frequency of heavy precipitation events will increase (Chen et al. 2009; Cheng et al. 2019), and this has been confirmed in studies of extreme precipitation in the Asia–Pacific (Choi et al. 2009), the India-Pacific (Caesar et al. 2011), the United States (Kunkel et al. 2003), western Africa (Aguilar et al. 2009), and other regions.

Changes in extreme precipitation within China are generally consistent with those of global precipitation change. However, extreme precipitation indexes show different trends. You et al. (2011) studied the characteristics of extreme precipitation events and found that the trend of total precipitation is increasing and that most extreme precipitation indexes are highly correlated with total precipitation in China. Furthermore, Zhai et al. (2005) found regional differences in changes in the extreme precipitation trend

in China. For example, the Yangtze River Basin, western China, and southeast coastal areas show increasing trends, whereas basins in northeast China, north China, and Sichuan province show decreasing trends.

Because of climate change from "warm and dry" regime to "warm and wet" regime in northwest China, it is necessary to understand the trend of regional climate change. The Qilian Mountains range from western Gansu Province to the northeastern border of Qinghai Province and are located at the intersection of three plateaus: the Qinghai–Tibet Plateau, the Inner Mongolia–Xinjiang Plateau, and the Loess Plateau (Gao et al. 2014; Li et al. 2016; Zhao et al. 2020). The mountains are known as the "lifeline" of the Hexi corridor. They lie within a typical climate-sensitive area and a fragile ecological environment zone. Therefore, the frequency and intensity of extreme climate events will inevitably have significant impacts on their ecological environment.

Recent studies on climate change in the Qilian Mountain area have focused on the temporal and spatial distribution of temperature. This study utilized 12 extreme temperature indexes and 12 extreme precipitation indexes based on daily temperature and precipitation data obtained from a long time series. A linear trend estimation method and a spline interpolation method were employed, in addition to correlation analysis, to analyze the characteristics of the temporal and spatial variations in the extreme temperature index and extreme precipitation index in the Qilian Mountain area from 1961 to 2017. The aims of this study were as follows. (1) To gain a deep understanding of the regional climate change trend under the background of a climate transformation from a warm and dry regime to a warm and wet one in northwest China. Furthermore, as the frequent occurrence and intensification of extreme climate events will inevitably have a significant impact on the ecological environment, we also aimed (2) to analyze the interannual variation and spatial distribution of the extreme temperature and precipitation indexes in the Qilian Mountain area, as well as (3) to discuss the relationship between elevation and the extreme temperature and precipitation indexes and evaluate the relationship between atmospheric circulation and these indexes. The findings could provide a scientific basis for comprehensively understanding the regional impacts of climate change.

Study areas and methods

Study area

The north, west, south, and southeast Qilian Mountain area is divided into the following areas: the Hexi corridor, Altun Mountains, the Qaidam Basin, Qinling Mountains, and Liupanshan Mountains, respectively. The Qilian Mountains (93.4°–103.4° E, 35.8°–40.0° N) lie in Gansu and Qinghai

Provinces. They have an average altitude of 4000–4500 m and are a transitional area between the northwest desert area and the alpine region of the Qinghai–Tibet Plateau. Qinghai Province is located far from the sea, and it has a typical continental and plateau climate. The eastern part of the study area is affected by the southeast and southwest monsoon (Gao et al. 2014; Li et al. 2016; Zhao et al. 2020), the westerly circulation controls the western part, and the central part lies at an intersection between these two types of circulation systems. Thus, the Qilian Mountain area has a complex climate (Gao et al. 2014; Li et al. 2016; Zhao et al. 2020), and the hydrothermal conditions differ throughout the area. The annual average temperature is 0.6 °C, and annual precipitation varies from 400 to 700 mm. There are many rivers within the Qilian Mountain area, and the vegetation distribution has unique vertical zonal characteristics. The soil system is also distinctly banded in a vertical direction.

Data sources and research methods

Daily temperature and precipitation data obtained from 24 meteorological stations (Fig. 1; Table 1) in the Qilian Mountain area from 1961 to 2017 were selected for analysis in the study. The meteorological data were obtained from the China Meteorological Data Network (http://data.cma.cn/). The extreme temperature indexes and extreme precipitation indexes defined in WMO (Peterson, 1998–2001) were used to define and calculate the extreme indexes. Twelve extreme temperature indexes (Table 2) and 12 extreme precipitation indexes (Table 3) were calculated using RClimDex software (Zhang et al. 2015). The data sets passed a quality control analysis prior to use and were determined to be uniform,

Table 1 The selected weather stations in Qilian Mountain area

| Station Number	Station Name	Latitude (°)	Longitude (°)	Altitude(m)
52,418	Dun Huang	40.09	94.41	1139.0
52,424	An Xi	40.32	95.46	1170.9
52,436	Yu Men Zhen	40.16	97.02	1526.0
52,447	Jin Ta	40.00	98.54	1270.5
52,533	Jiu Quan	39.46	98.29	1477.2
52,546	Gao Tai	39.22	99.50	1332.2
52,652	Zhang Ye	39.05	100.17	1461.1
52,661	Shan Dan	38.48	101.05	1764.6
52,674	Yong Chang	38.14	101.58	1976.9
52,679	Wu Wei	37.55	102.40	1531.5
52,797	Jing Tai	37.11	104.03	1630.9
52,876	Min He	36.20	102.50	1813.9
52,602	Leng Hu	38.45	93.20	2770.0
52,657	Qi Lian	38.11	100.15	2787.4
52,737	De Ling Ha	37.22	97.22	2981.5
52,765	Men Yuan	37.23	101.37	2850.0
52,856	Gong He	36.16	100.37	2835.0
52,866	Xi Ning	36.44	101.45	2295.2
52,868	Gui De	36.01	101.22	2237.1
52,633	Tuo Le	38.48	98.25	3367.0
52,645	Ye Niu Gou	38.25	99.35	3320.0
52,713	Da Chai Dan	37.51	95.22	3173.2
52,754	Gang Cha	37.20	100.08	3301.5
52,842	Cha Ka	36.47	99.05	3087.6
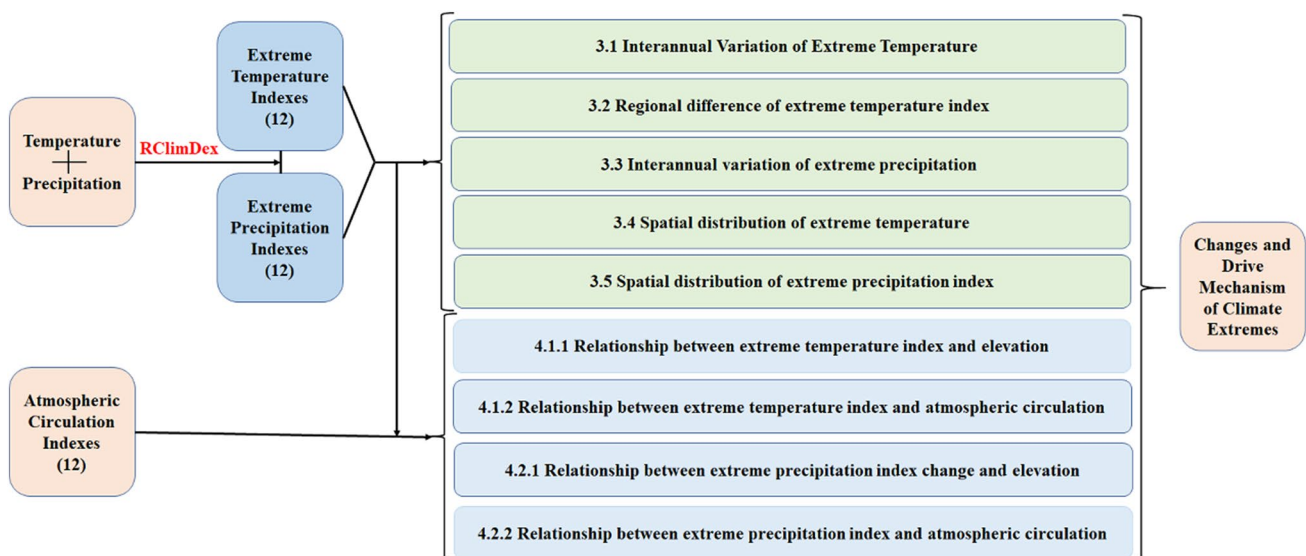
Fig.1 The flow chart of this study

Table 2 Definition of extreme temperature indexes and extreme precipitation indexes

Index Code	Name	Definition	Unit
TX10	Daytime Extreme Low Temperature Days	The number of days when the daily maximum temperature is less than the 10th percentile value in 1961–2017	d
TN10	Nighttime Extreme Low Temperature Days	The number of days when the daily minimum temperature is less than the 10th percentile value in 1961–2017	d
TXn	Lowest temperature of the daily maximum	The minimum value of daily maximum temperature of each month	°C
TNn	Lowest temperature of the daily minimum	The minimum daily temperature of each month	℃
TN90	Highest temperature days of nights	The number of days when the night minimum temperature is greater than the 90th percentile value in 1961–2017	d
TX90	Highest temperature days of daytime	The number of days when the daily maximum temperature is greater than the 90th percentile value in 1961–2017	d
TXx	Highest value of daily maximum temperature	Maximum daily maximum temperature of each month	°C
TNx	Highest value of daily minimum temperature	The maximum daily minimum temperature of each month	°C
ID	Freezing days	Days with daily maximum temperature lower than 0 °C	d
FD	Frost days	Days with daily minimum temperature below 0 °C	d
DTR	Daily temperature range	Difference between daily maximum temperature and minimum temperature in the year	°C
GSL	Growth season length	The total number of days when the daily average temperature is higher than 5 °C for at least 6 consecutive days and the total number of days when the average temperature is lower than 5 °C for at least 6 consecutive days after July 1	d
PRCPTOT	The total precipitation in the rain day	Total precipitation with daily precipitation greater than 1 mm	mm
SDII	Precipitation intensity in rainy days	Average rainfall on rainy days with daily precipitation greater than 1 mm	mm/d
RX1DAY	Maximum precipitation per day	Maximum precipitation per day in the year	mm
RX5DAY	Maximum precipitation in five days	Maximum precipitation for five consecutive days in the year	mm
R95	Extreme precipitation	The total precipitation in rainy days with daily precipitation greater than the 95th percentile	mm
R99	Very extreme precipitation	The total precipitation of rainy days with daily precipitation greater than the 99th percentile	mm
CDD	Number of continuous dry days	Continuous days with daily precipitation less than 1 mm	d
CWD	Number of continuous wet days	Continuous days with daily precipitation more than 1 mm	d
R10MM	Daily precipitation more than 10 mm days	Days with daily precipitation more than 10 mm	d
R20MM	Daily precipitation more than 20 mm days	Days with daily precipitation more than 20 mm	d
R25MM	Daily precipitation more than 25 mm days	Days with daily precipitation more than 25 mm	d
\	Rainy days	Days with daily precipitation greater than 1 mm	d

Table 3 Inter-annual trends of extreme temperature indexes in Qilian Mountain area

Index	1961–1969	1970–1979	1980–1989	1990–1999	2000–2009	2010–2017	1961–2017
TX10(d/10a)	5.75	2.17	1.15	− 2.94	1.29	**− 4.86**	**− 1.16**
TN10(d/10a)	− 1.81	− 1.51	− 2.14	− 4.49	− 1.20	**− 6.61**	**− 2.47**
TXN (°C/10a)	− 3.13	− 1.43	2.18	1.10	− 1.47	4.55	**0.36**
TNN (°C/10a)	2.13	− 0.62	1.43	2.02	− 0.42	4.09	**0.51**
ID (d/10a)	3.80	− 5.27	− 5.83	− 2.83	− 0.04	− 20.58	**− 3.30**
FD (d/10a)	− 5.39	− 3.63	− 7.42	**− 9.89**	**− 13.14**	**− 15.14**	**− 3.86**
DTR (°C/10a)	− 0.88	− 0.29	− 0.55	0.14	**− 0.51**	− 0.57	**− 0.16**
TN90(d/10a)	− 0.29	1.02	4.17	4.52	**6.21**	5.36	**2.39**
TX90(d/10a)	1.42	1.74	2.64	**8.61**	3.19	1.77	**1.68**
TXX (°C/10a)	− 1.28	− 0.95	0.10	2.65	**− 2.41**	− 0.12	**0.32**
TNX (°C/10a)	− 0.06	− 0.51	0.27	1.71	− 1.20	0.41	**0.42**
GSL (d/10a)	6.10	2.53	− 5.36	3.82	**13.14**	16.52	**3.48**

Bold words means passing the 95% confidence significance test

complete, and continuous from January 1, 1961 to December 31, 2017.

Twelve atmospheric circulation indexes were used to study the influences of circulation on extreme temperature variations in the Qilian Mountain area, including the Atlantic Multidecadal Oscillation (AMO), Tropical Northern Atlantic Index (TNA), Tropical Southern Atlantic Index (TSA), Northern Tropical Atlantic Index (NTA), Caribbean sea-level surface temperature (SST) Index (CAR), Northern Atlantic Oscillation (NAO), North Pacific model (NP), Arctic Oscillation (AO), Southern Oscillation Index (SOI), Multiple ENSO Index (MEI), and the South China Sea Summer Monsoon Index (SCSSMI). The SCSSMI was obtained from the NOAA Earth System Research Laboratory (https://www.esrl.noaa.gov/psd/data/climateindexes/list/).

When analyzing the trends in temporal variations of the extreme temperature and precipitation indexes, we used a linear regression equation to fit series variables. To determine whether the climate change trend was significant, it was necessary to test the correlation coefficient between the time and original sequence variables (Wei et al. 1999). A map of the spatial distribution of the climate element tendency rate change was drawn using ArcGIS software, and then, a spatial change analysis was conducted. The interpolation method of inverse distance weight (IDW) was subsequently used to analyze the spatial distribution of the extreme index. Inverse distance weighted interpolation relates to the square grid method multiplied by the reciprocal of distance. It is a weighted average interpolation method that can interpolate exactly or smoothly. The Pearson Correlation analysis method was also used to analyze the correlations between the extreme temperature and precipitation indexes and the atmospheric circulation indexes (Yu et al. 1999).

Results

Interannual variations in extreme temperature

As shown in Table 4, TX10 and TN10 showed overall significantly decreasing trends from 1961 to 2017, with decreasing rates of 1.16 d/10 a and 2.47 d/10 a, respectively, whereas TXN and TNN showed an increasing trend at rates of 0.36 °C/10 a and 0.51 °C/10 a, respectively. The interannual changes in the cold index of extreme temperature were similar. The study area experienced a warming climate in the mid-late 1980s. TX10, TN10, and TNN underwent significantly increasing trends in the 1990s. Although the warming decreased from 2000 to 2009, it increased significantly after 2010 (Fig. 2). Compared with the day index, the night index showed a larger warming range, and compared with the cold index, the warming index of extreme temperature showed an increasing trend (Fig. 2; Table 4). TN90 and TX90 increased

Table 4 Comparison between the linear trends in extreme temperature indexes in Qilian Mountain area and other regions

Index	TX10 (d/10a)	TN10 (d/10a)	TXN (°C/10a)	TNN (°C/10a)	TN90 (d/10a)	TX90 (d/10a)	TXX (°C/10a)	TNX (°C/10a)	ID (d/10a)	FD (d/10a)	DTR (°C/10a)	GSL (d/10a)	Data sources
Qilian Mountain area 1961–2017	**−1.16**	**−2.47**	**0.36**	**0.51**	**2.39**	**1.68**	**0.32**	**0.42**	**−3.3**	**−3.86**	**−0.16**	**3.48**	This study
China 1961–2008	**−3.26**	**−8.23**	**0.35**	**0.58**	**8.16**	**5.22**	**0.15**	**0.25**	**−2.32**	**−3.48**	**−0.15**	—	Zhou et al., 2011
Northwestern of China 1961–2012	−1.5	**−4.08**	—	0.46	**4.52**	**2.44**	0.17	—	—	—	**−0.21**	—	Zhao et al., 2017
Qinghai Tibet Plateau 1963–2012	**−2.75**	**−5.8**	—	**0.59**	**4.44**	**3.45**	**0.31**	—	**−1.86**	**−4.02**	**−0.15**	2.9	Zhao et al., 2014
Qingling 1960–2013	**−1.79**	**−2.05**	**0.38**	0.11	**2.24**	**2.59**	0.14	0.06	**−0.7**	**−3.01**	0.08	3.15	Zhang et al., 2018
Tianshan 1960–2015	**−1.23**	**−3.56**	0.29	**0.62**	**3.67**	**1.73**	0.09	**0.34**	**−1.16**	**−3.66**	**−0.25**	2.94	Ding et al., 2018
Mount Qomolangma 1971–2012	**−6.54**	**−8.87**	**0.37**	**0.64**	**12.07**	**8.17**	**0.3**	**0.4**	**−1.24**	—	**−0.08**	4.81	Du et al., 2014
Taonaihe 1957–2012	**−0.84**	**−1.13**	0.3	0.19	1.68	1.54	0.13	**0.25**	—	—	−0.01	—	Gao et al., 2014

Bold means passing the 95% confidence significance test, "–" indicates missing data

Fig. 2 The regional map and platform distribution of the Qilian Mountains
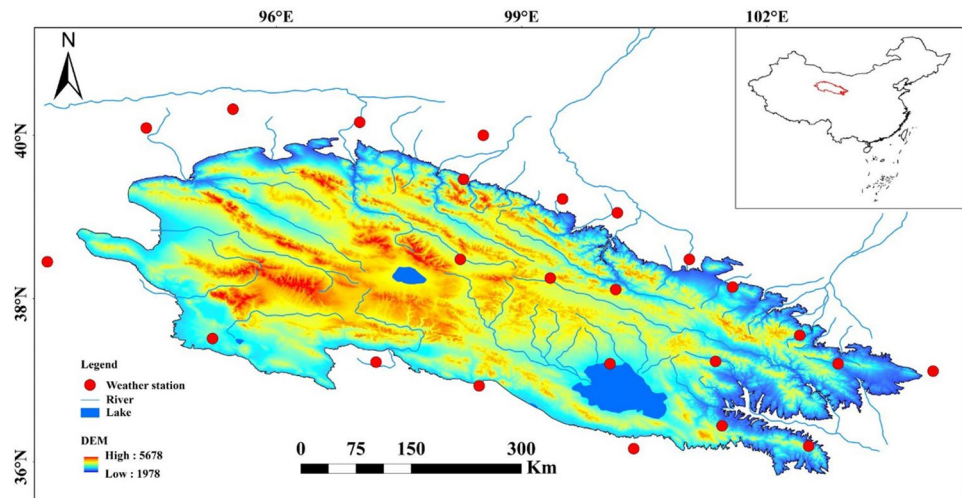
by rates of 2.39 d/10 a and 1.68 d/10 a from 1961 to 2017, respectively, and the results passed the significance level test. TXX and TNX increased significantly during the study period at rates of 0.32 °C/10 a and 0.42 °C/10 a, respectively.

The interannual change in the warming index of extreme temperature was similar to that of the cold index of extreme temperature. The climate of the study area was obviously warming after 1985, particularly during the 1990s. Although the TXX and TNX decreased from 2000 to 2009, they increased after 2010. The warming index of extreme temperature also confirmed that the warming range of the night index was larger than that of the day index. Compared with the cold index of extreme temperature, the change range of the warming index of extreme temperature was lower.

Over the study period, ice days (ID) and frost days (FD) decreased significantly by rates of 3.30 d/10 a and 3.86 d/10 a, respectively (Fig. 2). ID warmed continuously during the study period; FD warmed slightly prior to the mid and late

1980s and then warmed linearly. Diurnal temperature range (DTR) decreased significantly by 0.16 °C/10 a, which confirmed that the night index was warmer than the day index. Growing season length (GSL) increased significantly by 3.48 d/10 a, and the interannual change showed a fluctuating warming trend. Furthermore, a large linear warming trend was apparent after the mid and late 1980s.

Regional differences in the extreme temperature index

Table 5 shows the results of a comparison and analysis of changes in the extreme temperature index and its associated range between the Qilian Mountains and other regions in the same period. The analysis shows that the range of variation in the Qilian Mountains was consistent with that of China and other regions, but regional differences were also apparent. For example, the cold indexes of TX10, TN10,

Table 5 The annual trends of extreme precipitation indexes in Qilian Mountain area and basins

Index	PRCPTOT		SDII		RX1DAY		RX5DAY		R95		R99	
	mm/10a	%	mm/d/10a	%	mm/10a	%	mm/10a	%	mm/10a	%	mm/10a	%
Qilian Mountain	**13.86**	41.8	− 0.01	3.8	**0.76**	27.2	**1.37**	31.9	**4.10**	72.8	**1.29**	66.1
Hexi Corridor	**10.51**	47.8	− 0.02	3.8	**0.81**	31.1	**1.11**	33.0	**3.60**	92.6	**1.10**	78.2
Qaidam Basin	**14.05**	43.3	0.01	8.3	**0.75**	33.5	**1.97**	44.0	**4.48**	97.7	**1.60**	153.5
Yellow River	**24.40**	33.6	− 0.03	− 2.4	0.63	12.5	1.17	17.4	**5.06**	34.4	1.39	6.5
Index	CDD		CWD		R10MM		R20MM		R25MM		Rainy day	
	d/10a	%	d/10a	%	d/10a	%	d/10a	%	d/10a	%	d/10a	%
Qilian Mountain	**− 26.35**	− 49.0	0.06	12.6	**0.40**	47.0	**0.09**	62.9	**0.05**	64.6	**5.79**	43.5
Hexi Corridor	**− 26.74**	− 50.2	0.05	15.7	**0.28**	57.4	**0.07**	93.2	**0.04**	87.5	**4.00**	47.6
Qaidam Basin	**− 24.42**	− 42.0	**0.10**	14.6	**0.43**	48.4	**0.11**	89.2	**0.05**	125.0	**4.20**	37.4
Yellow River	**− 28.43**	− 59.0	0.01	5.3	**0.75**	35.8	0.12	26.0	0.06	18.6	**7.93**	42.2

Bold means passing the 95% confidence significance test

and TNN in the Qilian Mountains were smaller than those in other areas, while ID and FD were larger than those in other areas. However, there was no significant difference in TXN. TXX, TNX, and GSL were larger than those in other areas, and TX90 and TN90 were smaller than those in other areas. DTR was slightly larger than that of the whole country (Zhou et al. 2011), the Qinghai-Tibet Plateau (Zhao et al. 2014), and Mount Everest (Du et al. 2016) but smaller than that of northwest China (Zhao et al. 2017) and the Tianshan Mountains (Ding et al. 2018). It is also of note that the relative indexes (TX10, TN10, TX90, and TN90) were far smaller than those of the whole country, northwest China, the Qinghai–Tibet Plateau, the Tianshan Mountain area, and Mount Everest but larger than those of the Qilian Mountains and the Taolai River Basin (Gao et al. 2014) (which was not significantly different from that of the Qinling Mountains) (Zhang et al. 2018). In general, the cold indexes (ID and FD) and warming indexes (TXX, TNX, and GSL) were larger in the Qilian Mountains than in other areas, and they showed that extreme low-temperature events in the Qilian Mountains were less frequent than that in other areas. However, extreme high-temperature events occurred more frequently in the Qilian Mountains than in other areas, and the climate warming trend was more noticeable.

Interannual variations in extreme precipitation

Wet day precipitation (PRCPTOT), simple daily intensity index (SDII), maximum 1-day precipitation (RX1DAY), maximum 5-day precipitation (RX5DAY), very wet day precipitation (R95), and extremely wet day precipitation (R99) in the Qilian Mountain area changed by 13.86, − 0.01, 0.76, 1.37, 4.10, and 1.29 mm/d/10 a from 1961 to 2017, respectively. More importantly, all the extreme precipitation indexes (with the exception of the SDII) passed the 5% significance level test. The PRCPTOT, SDII, RX1DAY, RX5DAY, R95, and R99 increased by 41.8%, 3.8%, 27.2%, 31.9%, 72.8%, and 66.1%, respectively. There were increases in the extreme precipitation indexes of the three basins associated with the Qilian Mountain area, with the exception of the SDII in the Yellow River Basin; the extent of increase in the extreme precipitation indexes was lower in the Yellow River Basin than in the Qilian Mountains. The Inland River Basins in Hexi and Qaidam were higher than, or equivalent to, those of the Qilian Mountains (Table 6).

As shown in Fig. 3, interannual variations in PRCPTOT, RX5DAY, and R95 indexes in the Qilian Mountains underwent significant increases in the 1980s and from 2000 to 2017, but only slight increases (and at times decreases) during the 1990s. The trends of the SDII, RX1DAY, and R99 indexes were relatively stable, but the extent of their increase grew after 2010. The trends of the PRCPTOT, SDII, RX1DAY, R95, R99, and RX5DAY indexes in the Hexi

Table 6 Correlation coefficients between elevations and linear trends of extreme temperature indexes from 1961to 2017 in Qilian Mountain area

Index	$b(\times 10^6)$	R^2	Index	$b(\times 10^6)$	R^2
TX10	**− 26.63**	0.51	DTR	− 5.37	0.06
TN10	**− 68.45**	0.22	TN90	− 11.65	0.02
TXN	**11.03**	0.44	TX90	− 5.87	0.02
TNN	**21.52**	0.22	TXX	− 1.24	0.01
ID	**− 131.20**	0.68	TNX	− 3.18	0.05
FD	**− 85.94**	0.20	GSL	10.86	0.01

Bold means passing the 95% confidence significance test

Inland River Basin were all relatively stable, but all indexes except the RX5DAY showed an increasing trend after 2010. Interannual variations in the PRCPTOT, RX5DAY, and R95 indexes within the Qaidam Inland River Basin increased significantly in the 1980s and from 2000 to 2017 but decreased during the 1990s, and SDII, RX1DAY, and R99 maintained stable trends but increased considerably after 2010. Interannual variations in the PRCPTOT and R95 indexes within the Yellow River Basin increased significantly in the 1980s and from 2000 to 2017 but decreased during the 1990s, and SDII, RX1DAY, and RX5DAY maintained a stable trend but increased slightly after 2000. Furthermore, R99 increased significantly from 1980 to 1999 and from 2010 to 2017, while only increasing slightly from 2000 to 2009.

Rainy days, consecutive wet days (CWD), R10MM, R20MM, and R25MM increased by 5.79 d/10 a, 0.06 d/10 a, 0.40 d/10 a, 0.09 d/10 a, and 0.05 d/10 a, respectively. All daily indexes of extreme precipitation except CWD passed the significance level test of 5%. The percentage increases in rainy days, CWD, R10MM, R20MM, and R25MM were 43.5%, 12.6%, 47.0%, 62.9%, and 64.6%, respectively. All daily indexes of extreme precipitation [except for consecutive dry days (CDD)] in the Hexi Inland River Basin, Qaidam Inland River Basin, and Yellow River Basin showed increasing trends. Compared to the Qilian Mountains, the extents of the increases in CWD, R10MM, R20MM, and R25MM were lower in the Yellow River Basin but higher in the Hexi Inland River Basin and Qaidam Inland River Basin (Table 6). Rainy days, R10MM, R20MM, and R25MM in the Qilian Mountains, Qaidam Inland River Basin, and Yellow River Basin increased significantly in the 1980s and after 2010 but decreased in the 1990s. Rainy days in the Hexi Inland River Basin showed a decreasing trend in the 1990s, and it increased steadily in other years, whereas R10MM, R20MM, and R25MM showed relatively stable increases and significant increases after 2010. The CWD index in the Qilian Mountains, Hexi Inland River Basin, and Qaidam Inland River Basin decreased from 1980 to 1999
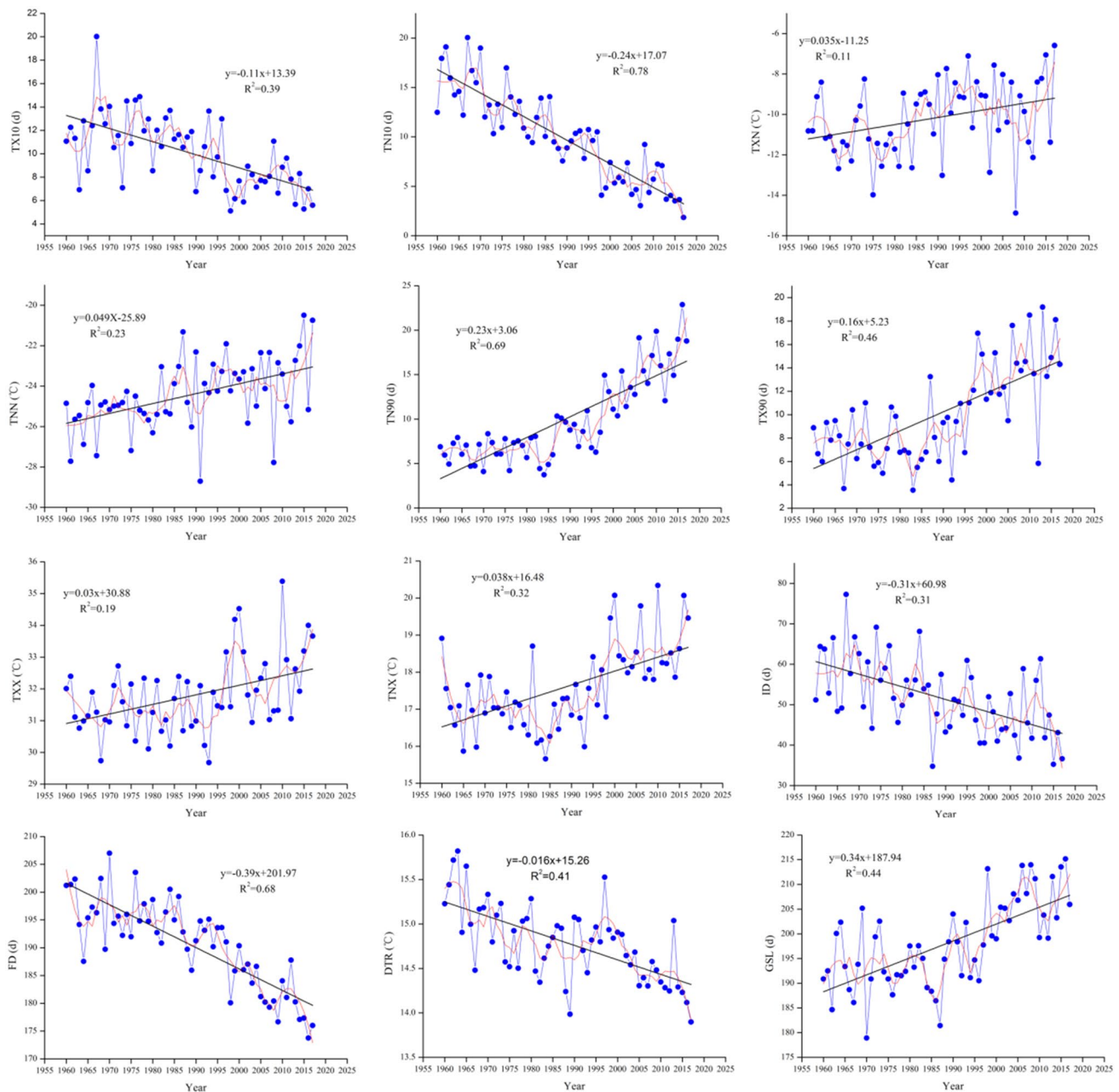
Fig. 3 The annual variation curves of extreme temperature in Qilian Mountains from 1961 to 2017

but increased after 2000. Although it maintained a stable trend in the Yellow River Basin, the CWD index increased after 2000. CDD decreased significantly by a rate of 26.35 d/10 a, with a reduction rate of 49%. Compared to the Qilian Mountains, the reductions in the Yellow River Basin and Hexi Inland River Basin were greater, but the rate of reduction was lower in the Qaidam Inland River Basin. Interannual changes in the Qilian Mountains and the three basins decreased significantly in the 1980s but increased significantly in the 1990s. After 2000, the Qaidam Inland River Basin and Yellow River Basin showed decreasing

trends, but in the Hexi Inland River Basin, the CDD increased significantly after 2010 (Fig. 3).

Spatial distribution of extreme temperature

As shown in Fig. 4, the warming amplitude of TX10 at 24 stations passed the significance level test, and the warming amplitude of TN10 passed the significance test at all stations except Xining station. TXN and TNN at all stations showed a warming trend, but the significance level test was only passed at 42% and 58% of the stations, respectively. Such
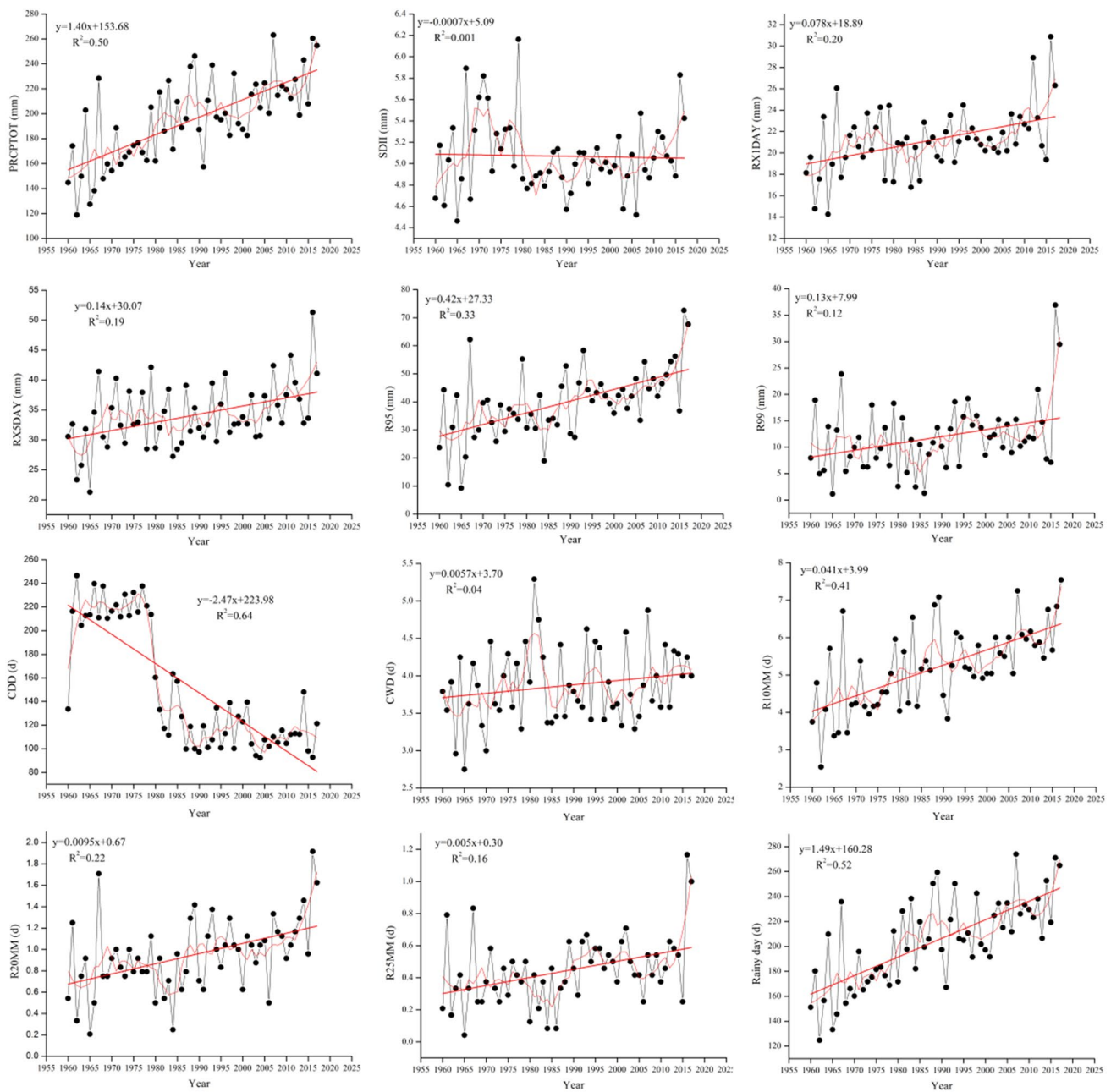
Fig. 4 The annual variation curves of extreme precipitation in Qilian Mountains from 1961 to 2017

stations were located mainly in an area with a large warming range. In general, the warming range of the four indexes (TX10, TN10, TXN, and TNN) decreased from south to north.

As shown in Fig. 4, 60–100% of all stations showed significant warming trends. The TN90 and TNX of all stations (except Xining) showed a warming range (Fig. 4) at a significant level. For TX90, a significant warming trend was observed at 24 stations. TXX showed a warming trend at all stations, but a significant level was only seen at 67% of stations, most of which were located in an area with a large

warming range. For these four indexes, a small warming range occurred in the middle and eastern Qilian Mountain area, and TN90 and TNX increased in a ring while TX90 and TXX increased in a band.

The ID and FD of all stations showed a warming trend (Fig. 4), and the trend was significant at all stations (except at Dunhuang and Xining stations for ID and FD, respectively). The warming trends of ID and FD decreased from south to north within the Qilian Mountain area. For DTR, 92% of stations showed a decreasing trend that was significant at 75% of stations. However, Yumen and Xining stations

showed significant increasing trends, which may relate to the acceleration of the urbanization process and changes made to underlying surface properties, which has resulted in a higher day index heating rate compared to that of the night index (Lin et al. 2017). For GSL, the significance level test was passed at 24 stations; although the spatial distribution of GSL was low in the middle and eastern Qilian Mountain area, it increased from inside to outside.

Spatial distribution of extreme precipitation index

As shown in Fig. 5, spatial distributions of PRCPTOT, SDII, RX1DAY, RX5DAY, R95, and R99 were similar throughout the Qilian Mountain area. Although the central Qilian

Mountain area showed the largest increase in these spatial distributions, the region of increase in spatial distribution decreased from the inside to the outside. The PRCPTOT of all stations showed an increasing trend that was significant at 17 stations. Stations with no significant increasing trend were mainly located on the edge of the Qilian Mountain area, and the increased trend in such regions was small. Yeniugou station, in the middle of the Qilian Mountain area, showed the largest increasing trend, reaching 45.57 mm/10 a. The SDII of 11 stations showed an increasing trend, and these were mainly located in the Qaidam Inland River Basin. Only the tole station showed a significant increase, and this indicated that precipitation increases in this area may result from an increase in the precipitation intensity. Stations with
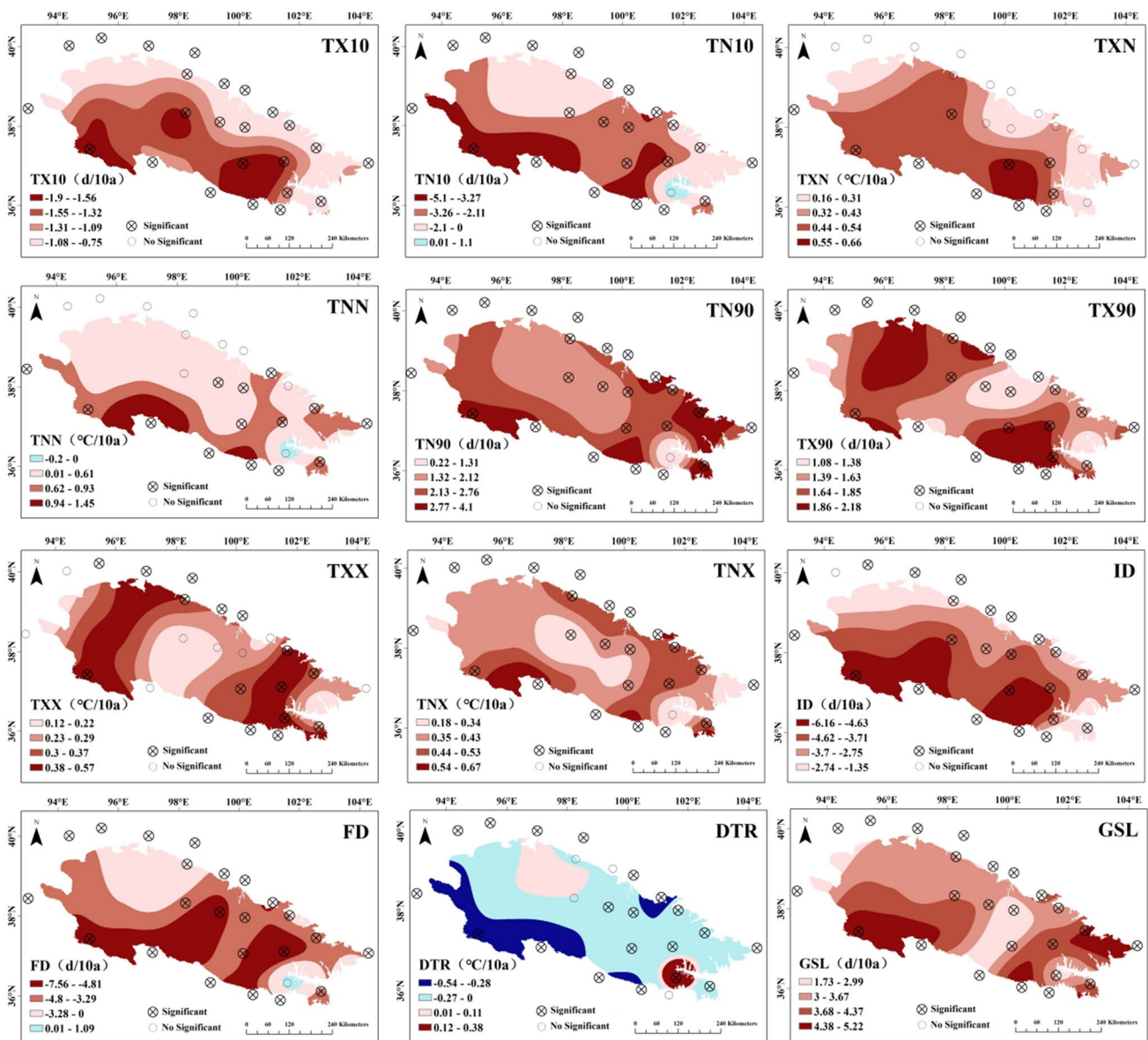

Fig.5 Spatial distribution of change ranges of extreme temperature in Qilian Mountains from 1961to 2017

a decreasing SDII trend were mainly located in the eastern and western Qilian Mountain area, but only the decreasing trend at Minhe station passed the significance level test (Fig. 6).

RX1DAY and RX5DAY showed increasing trends at 19 and 21 stations, respectively. Stations with significant increasing trends were mainly located in the middle of the Qilian Mountain area, while stations with decreasing trends were mainly located in the eastern part of the Qilian Mountain area. Compared with RX1DAY, the areas with a large increasing range of RX5DAY were concentrated in the Qaidam Inland River Basin. R95 and R99 showed similar trend changes, as well as increasing trends at 19 stations, with significance being achieved at six stations that were

mainly located in the middle of the Qilian Mountains. R95 and R99 of five stations showed a decreasing trend, and these were mainly located in the eastern part of the Qilian Mountain area. Compared with R95, R99 showed a significant increasing trend in the eastern region.

The spatial changes in R10MM, R20MM, R25MM, and rainy days were similar to those of the extreme precipitation index. The central part of the Qilian Mountain area showed a large region, wherein these indexes exhibited an increasing trend, but the region of increase in these indexes decreased from the inside to the outside. There were increasing R10MM, R20MM, and R25MM trends at more than 20 stations, and stations in areas of significant increase were mainly located in the middle of the Qilian Mountain area.
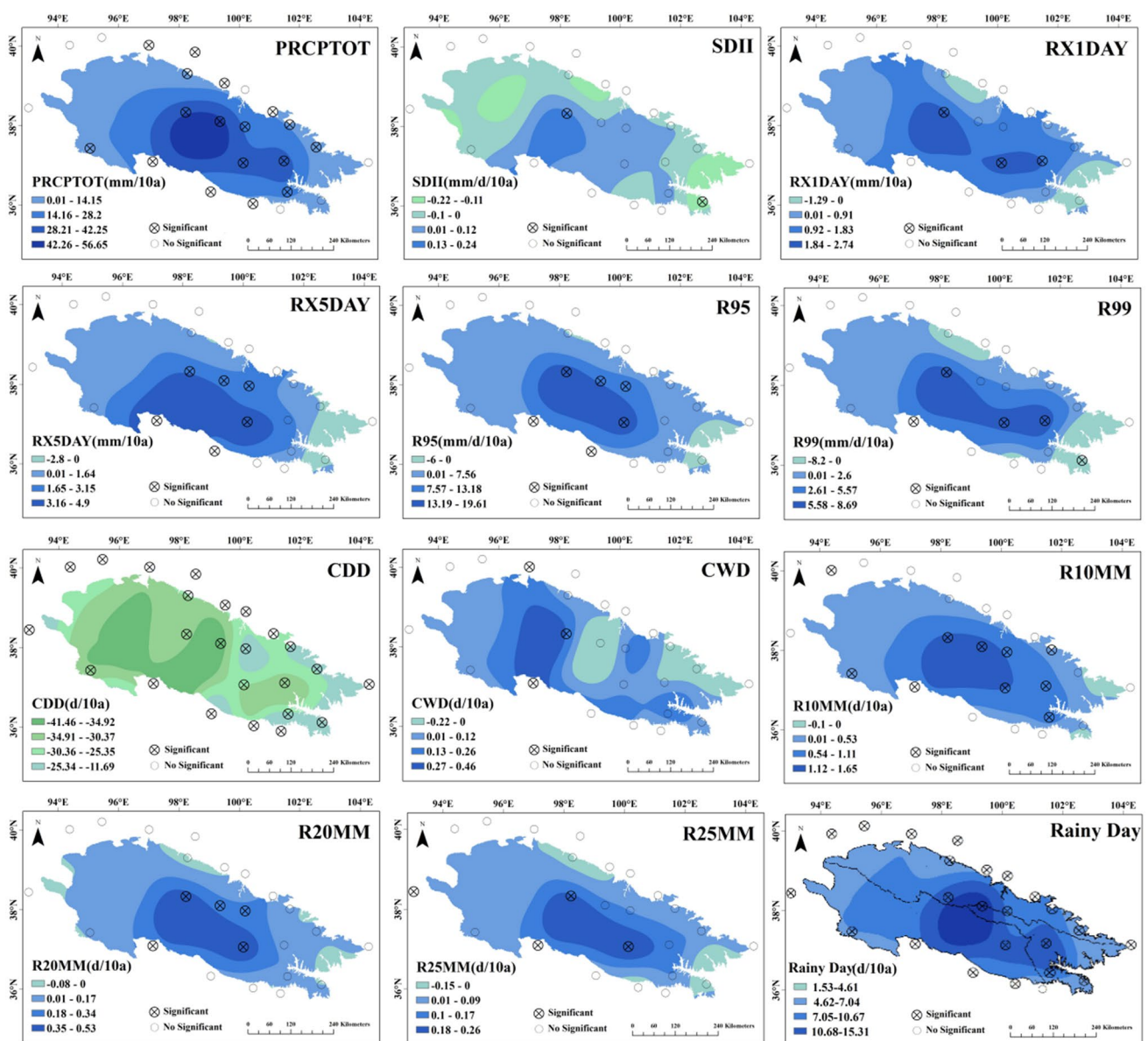

Fig. 6 Spatial distribution of change ranges of extreme precipitation indexes in Qilian Mountains and basins from 1961to 2017

In contrast, stations with decreasing trends were mainly located in the eastern Qilian Mountain area. The number of rainy days at all stations showed an increasing trend that was significant at all stations (except Guide station). Yeniugou station is located in the middle of the Qilian Mountain area, and it showed the largest increase of 13.26 d/10 a. The 24 stations that estimated CDD showed significant decreasing trends, and these stations were spatially distributed in the central and western Qilian Mountain area, and the range of decrease was minimized to the east. The CWD of 19 stations showed an increasing trend that passed the significance test at three stations that were mainly located in the western part of the Qilian Mountain area. There was a decreasing trend at five stations that were mainly located in the middle and eastern parts of the Qilian Mountain area, but these trends failed to pass the 5% significance level test.

Global warming is accelerating the water cycle, and this is resulting in an increased frequency of extreme climate events; extreme warm events and extreme heavy precipitation events are increasing in most land areas. Since the early 1950s, the global average surface temperature has increased by 0.12 °C/10 a and that in China has increased by 0.25 °C/10 a in the past few decades (Stocker et al. 2014). The number of frost days is declining in most parts of the world, and the decline in the trend is faster in Europe and Asia than in other parts of the world. The trend is most noticeable in Northern Europe but is less apparent in North America and Australia. The number of ice days is also decreasing in most parts of the northern hemisphere, especially in central and Northern Europe (Zhang et al. 2020). However, Folland et al. (2001) found a cooling trend in summer from 1976 to 2000 in the central United States. Pan et al. (2004) called the cooling phenomenon in this area a "warm hole", and believed that low-level atmospheric circulation may supply greater amounts of soil moisture in summer that resulted in increased evaporation, which inhibited the daily maximum temperature in summer. From 1980 to 2019, the warming rate of the average surface temperature was approximately 0.56 °C/10 a in the Arctic, where significant global warming is evident (Meredith et al. 2019). The frequency and intensity of extreme warm events have increased significantly, while the frequency and intensity of cold events has decreased (Sui et al. 2017). Overall, the warming rate in the Qilian Mountain area was lower than that in other regions.

Discussion

Factors influencing the extreme temperature index

Relationship between extreme temperature index and elevation

As shown in Table 7, the rate of extreme temperature index change in the Qilian Mountain area has a good statistical relationship with altitude. The correlation coefficients of TX10, TN10, TXN, TNN, ID, FD, and altitude passed the significance level test of 0.05. TX10, TN10, ID, and FD showed a significant negative correlation with altitude, while TXN and TNN showed a significant positive correlation with altitude. For every 100-m increase in elevation, TX10, TN10, ID, and FD decreased by 0.03 d/10 a, 0.07 d/10 a, 0.13 d/10 a, and 0.09 d/10 a, respectively, whereas TXN and TNN increased by 0.01 °C/10 a and 0.02 °C/10 a. With respect to altitude, the warming range of the night index (TNN and TN10) was larger than that of the day index (TXN and TX10).

The linear trends of the extreme temperature indexes at different elevations in the Qilian Mountain area from 1961 to 2017 are shown in Table 8, wherein it is evident that change characteristics of each index differ. For example, changes in TX10, TN10, TXN, TNN, ID, FD, and DTR were the most obvious in high-altitude areas (> 2500 m), and changes in TN90, TX90, TXX, TNX, and GSL were the most obvious in low altitude areas (< 2500 m). The results also show that changes in the cold index and other indexes were the most obvious in high-altitude areas. The change in the warm index was the most sensitive in low altitude areas, and the characteristics were similar to those of the relationship between the extreme temperature index and altitude in Tibet (Du et al. 2013) and the southwestern area (Li et al. 2012).

Relationship between extreme temperature index and atmospheric circulation

The Pearson Correlation analysis method was used to establish the correlation between the extreme temperature index and the circulation index, with the aim of understanding the relationship between the extreme temperature index and the circulation index of the Qilian Mountain area (Table 9). AMO, TNA, TSA, NTA, and CAR are indexes that reveal the SST of the Atlantic Ocean. AMO is a long-period interdecadal SST anomaly rate mode provided on a basin scale in the North Atlantic region (Folland et al. 1986; Delworth et al. 2000), and it showed the strongest correlation with each other extreme temperature

Table 7 Linear trends of extreme temperature and precipitation indexes of different elevations from 1961to 2017 in Qilian Mountain area

Elevation(m)	TX10	TN10	TXN	TNN	ID	FD
1000–1500	**− 1.01**	**− 1.98**	0.27	0.18	**− 2.15**	**− 3.21**
1500–2000	**− 0.91**	**− 2.09**	0.29	**0.58**	**− 2.59**	**− 3.7**
2000–2500	**− 1.19**	**− 0.93**	**0.44**	**0.23**	**− 2.72**	**− 1.26**
2500–3000	**− 1.3**	**− 3.71**	**0.44**	**0.89**	**− 4.6**	**− 5.05**
3000–3500	**− 1.49**	**− 2.9**	**0.46**	**0.57**	**− 4.46**	**− 4.78**
Elevation(m)	DTR	TN90	TX90	TXX	TNX	GSL
1000–1500	**− 0.11**	**2.31**	**1.78**	**0.31**	**0.48**	**3.05**
1500–2000	**− 0.17**	**2.91**	**1.57**	**0.32**	**0.43**	**3.92**
2000–2500	**0.15**	**1.19**	**2.06**	**0.52**	**0.27**	**3.37**
2500–3000	**− 0.31**	**2.45**	**1.54**	**0.3**	**0.46**	**3.52**
3000–3500	**− 0.19**	**2.28**	**1.68**	**0.28**	**0.37**	**3.49**
Elevation(m)	PRCPTOT	SDII	RX1DAY	RX5DAY	R95	R99
1000–1500	**4.29**	− 0.04	0.4	0.82	0.63	− 0.03
1500–2000	**7.47**	− 0.07	0.7	0.56	2.36	− 0.16
2000–2500	**11.56**	0.02	0.11	0.6	1.42	0.71
2500–3000	**19.36**	0.01	**0.93**	**2.04**	**5.17**	**2.29**
3000–3500	**28.41**	0.05	**1.34**	**2.64**	**10.35**	**3.86**
Elevation(m)	CDD	CWD	R10MM	R20MM	R25MM	Rainy day
1000–1500	**− 26.94**	0.05	0.12	0	0.01	**2.77**
1500–2000	**− 24.83**	0	0.13	0.05	0.02	**3.78**
2000–2500	**− 15.98**	0.06	0.46	0.04	0.05	**3.59**
2500–3000	**− 27.04**	0.11	**0.61**	**0.12**	0.06	**5.34**
3000–3500	**− 30.89**	0.08	**0.84**	**0.25**	**0.12**	**7.99**

Bold means passing the 95% confidence significance test

indexes at a significant level. The Nino4 is an SST index for the central tropical Pacific Ocean. Compared with the warm index, it was significantly correlated with the cold extreme temperature index in the Qilian Mountain area. The four major waves (NAO, NP, SOI, and AO) cover most of the global ocean area and have an important impact on the climate of adjacent land. However, their correlations with the extreme temperature index were not significant in the Qilian Mountain area. SOI and MEI are indexes of ENSO, and there was no significant correlation with any other index. Compared with the cold index, the correlation between SCSSMI and extreme air temperature indexes was significant. Both AMO and SCSSMI were positively correlated with TX10, TN10, ID, FD, and DTR, and other extreme temperature indexes. TNA, TSA, NTA, CAR, and Nino4 indexes were negatively correlated with AMO, SCSSMI, and extreme temperature indexes.

Factors influencing the extreme precipitation index

Relationship between changes in the extreme precipitation index and elevation

The Qilian mountain area can be divided into the Mountain area, the Hexi Inland River Basin, the Qaidam Inland River Basin, and the outflow area, according to the distribution of runoff. Table 10 shows the results of correlation analyses between the change range of the extreme precipitation index and elevation in the Mountain area, the Hexi Inland River Basin, the Qaidam Inland River Basin, and the outflow area. The correlation coefficient between all extreme precipitation indexes (except CDD and CWD) and altitude in the Mountain area and the Hexi Inland River Basin passed the significance level test. However, the correlation between the change range of the extreme precipitation index and altitude in the Mountain area was lower than that in the Hexi Inland River Basin. The correlation coefficients of RX1DAY, CDD, and rainy days with elevation passed the significance level test in the Qaidam Inland River Basin, and the correlation coefficients of PRCPTOT, R95, CDD, R10MM, and rainy days with altitude passed the significance level test in the outflow area. Compared with the Mountain area and Hexi Inland River Basin, the correlation between extreme precipitation index and altitude was relatively low at widely distributed stations in the Qaidam Inland River Basin and the outflow area (4 stations). Stations in the Qaidam Inland River Basin were distributed between 2500 and 3500 m above sea level.

There was a significant positive correlation between altitude and PRCPTOT, RX1DAY, RX5DAY, R95, R99,

Table 8 Correlation coefficients between extremes temperature and precipitation index and atmospheric circulation index in Qilian Mountain area

Index	TX10	TN10	TXN	TNN	ID	FD	DTR	TN90	TX90	TXX	TNX	GSL
AMO	**0.34**	**0.42**	**−0.29**	**−0.39**	**0.34**	**0.52**	**0.4**	**−0.54**	**−0.39**	**−0.35**	**−0.37**	**−0.38**
TNA	**−0.45**	**−0.45**	0.17	0.26	**−0.39**	**−0.52**	−0.13	**0.59**	**0.61**	**0.36**	**0.55**	**0.49**
TSA	**−0.41**	**−0.49**	0.23	**0.26**	**−0.36**	**−0.5**	−0.22	**0.48**	**0.54**	**0.3**	**0.33**	**0.47**
NTA	**−0.5**	**−0.55**	0.23	**0.34**	**−0.44**	**−0.59**	−0.23	**0.64**	**0.63**	**0.35**	**0.55**	**0.53**
CAR	**−0.69**	**−0.64**	**0.35**	**0.35**	**−0.51**	**−0.72**	−0.26	**0.77**	**0.67**	**0.43**	**0.6**	**0.68**
Nino 4	**−0.3**	**−0.28**	**0.33**	**0.41**	**−0.42**	−0.23	−0.05	**0.28**	**0.3**	−0.04	0.07	**0.27**
NAO	0.04	−0.08	0.24	0.12	−0.02	−0.02	−0.19	−0.07	−0.15	−0.05	−0.11	−0.02
NP	0	0.03	−0.08	−0.15	0.08	−0.12	−0.04	0.09	0.07	0.01	0.02	0.09
AO	−0.12	−0.22	0.17	0.02	−0.1	−0.24	**−0.34**	0.15	−0.05	0	0.03	0.2
SOI	0.09	0.2	−0.05	−0.24	0.16	0.18	0.17	−0.1	−0.1	0.09	0.01	−0.08
MEI	−0.24	−0.21	**0.29**	**0.36**	**−0.39**	−0.12	0.01	0.14	0.18	−0.11	−0.13	0.18
SCSSMI	**0.29**	**0.47**	−0.17	−0.24	**0.37**	**0.4**	**0.3**	**−0.41**	**−0.4**	**−0.32**	**−0.38**	**−0.27**
Index	PRCPTOT	SDII	RX1DAY	RX5DAY	R95	R99	CDD	CWD	R10MM	R20MM	R25MM	Rainy day
AMO	**−0.38**	−0.17	**−0.3**	**−0.3**	**−0.44**	**−0.37**	0.2	−0.16	**−0.38**	**−0.45**	**−0.39**	**0.34**
TNA	**0.3**	−0.02	0.22	0.25	**0.26**	**0.3**	**−0.41**	0.04	**0.28**	0.21	0.19	0.14
TSA	**0.3**	−0.14	0.09	0.13	0.12	0.12	−0.38	−0.02	0.24	0.13	0.07	0.21
NTA	**0.41**	−0.04	**0.26**	**0.3**	**0.33**	**0.32**	**−0.55**	0.07	**0.38**	0.24	0.23	**0.45**
CAR	**0.42**	−0.07	**0.26**	0.22	**0.35**	**0.35**	**−0.49**	0.08	**0.37**	**0.32**	**0.35**	**0.31**
NINO4	0.11	−0.14	0	0.02	0.1	−0.01	**−0.39**	0.03	0.09	0.04	0.04	**−0.01**
NAO	0.19	0.11	0	0.06	0.19	0	−0.21	0.1	0.22	0.16	0.16	−0.21
NP	−0.11	0.05	0.06	0	−0.08	0.02	0.21	−0.04	−0.11	0.01	0.06	0.22
AO	**0.33**	0.01	0.09	0.14	**0.26**	0.07	−0.29	0.17	**0.31**	**0.28**	0.24	**0.27**
SOI	0.05	0.18	0.13	0.16	0.09	0.14	0.2	0.06	0.07	0.15	0.1	0.12
MEI	0.12	−0.16	0	−0.02	0.05	−0.04	**−0.39**	0.02	0.08	−0.04	−0.03	0.03
SCSMI	**−0.4**	−0.02	−0.23	**−0.29**	**−0.27**	−0.24	**0.38**	−0.14	**−0.38**	−0.19	−0.13	**0.32**

Bold means passing the 95% confidence significance test

Table 9 Correlation coefficients between elevations and linear trends of extreme precipitation indexes from 1961 to 2017 in Qilian Mountain area and basins

Sites	PRCPTOT	SDII	RX1DAY	RX5DAY	R95	R99
Mountain area	**0.74**	**0.48**	**0.43**	**0.60**	**0.68**	**0.55**
Hexi Inland River Basin	**0.98**	**0.68**	**0.65**	**0.69**	**0.96**	**0.83**
Qaidam inland river basin	0.65	0.20	**0.80**	0.66	0.73	0.60
Outflow area	**0.99**	0.71	0.76	0.93	**0.98**	0.81
Sites	CDD	CWD	R10MM	R20MM	R25MM	Rainy day
Mountain area	−0.24	0.24	**0.73**	**0.64**	**0.56**	**0.66**
Hexi Inland River Basin	−0.19	0.50	**0.95**	**0.91**	**0.86**	**0.95**
Qaidam inland river basin	**−0.77**	0.57	0.53	0.63	0.54	**0.82**
Outflow area	**−0.99**	−0.75	**0.96**	0.93	0.86	**0.99**

Bold means passing the 95% confidence significance test

R10MM, R20MM, R25MM, and rainy days in the Mountain area Hexi Inland River Basin, as well as a significant positive correlation between altitude and the RX1DAY and rainy days in the Qaidam Inland River Basin. There was a significant positive correlation between altitude and PRCPTOT, R95, R10MM, and rainy days in the outflow area. These results reflect the more obvious increase in precipitation and rainy days in the high-altitude area. More importantly, the significant positive correlation between altitude and SDII in the Mountain area and the Hexi Inland River Basin reflect

the decrease in the precipitation intensity with an increase in altitude. However, the CDD shows a significant negative correlation with altitude in the Qaidam Inland River Basin and the outflow area, which reflects the decrease in the number of continuous dry days that has mainly occurred in the high-altitude area. For every 100 m increase in elevation, the decrease in SDII in the Mountain area decreased by 0.01 mm/d/10 a, and the increase in PRCPTOT, RX1DAY, RX5DAY, R95, R99, R10MM, R20MM, R25MM, and rainy days increased by 1.23 mm/10 a, 0.04 mm/10 a, 0.10 mm/10 a, 0.44 mm/d/10 a, 0.20 mm/d/10 a, 0.04 d/10 a, 0.01 d/10 a, 0.01 d/10 a, and 0.25 d/10 a, respectively.

Table 11 shows the range of extreme precipitation index change at different altitudes in the Qilian Mountain area. The range of extreme precipitation index change was relatively large in the high-altitude area (> 2500 m), except for that of SDII. There were 10 stations located above 2500 m in the Qilian Mountain area, of which six were located in the Qaidam Inland River Basin (Table 1). The change range of the extreme precipitation index was the most obvious in the Qaidam Inland River Basin.

Relationship between the extreme precipitation index and atmospheric circulation

As shown in Table 12, the correlation of the extreme precipitation indexes of the Mountain area, Hexi Inland River Basin, and Qaidam Inland River Basin was higher, but that of the outflow area was lower. AMO is a long-period interdecadal sea surface temperature anomaly rate mode provided on a basin scale in the North Atlantic region (Folland et al. 1986; Delworth et al. 2000), and it showed the highest correlation with the extreme precipitation index of the Mountain area and Qaidam Inland River Basin and the extreme precipitation day index of the Hexi Inland River Basin. NTA had a high correlation with extreme precipitation index in the Mountain area and in the Qaidam Inland River Basin. CAR had a high correlation with extreme precipitation index in the Mountain area and the Hexi Inland River Basin, and it was highly correlated with each extreme precipitation index in the Qaidam Inland River Basin. Nino4 is the SST index of the middle tropical Pacific Ocean, and it showed a low correlation with the extreme precipitation index of the Mountain area and of the three basins. The four major waves (NAO, NP, SOI, and AO) cover most of the global ocean area and have an important impact on the climate of the adjacent land. The correlation between the four waves and the extreme precipitation index was insignificant in the Mountain area, the Hexi Inland River Basin, and the Qaidam inland river basin. However, the correlation between AO and the extreme precipitation day index was high in the outflow area. SOI and MEI are the indexes of ENSO, and they were not found to be significantly correlated with the extreme precipitation

indexes in the Mountain area and the three basins. SCSSMI was highly correlated with the extreme precipitation index in the Qaidam Inland River Basin, the outflow area, the Mountain area, and the Hexi Inland River Basin. Furthermore, South American Summer Monsoon Index (SAMSMI) was correlated with the extreme precipitation index in the Mountain area and the Qaidam Inland River Basin, but there were no correlations with the extreme precipitation index in the Hexi Inland River Basin and the outflow area.

The AMO, NTA, and CAR indexes in the Mountain area and the three basins were negatively correlated with SDII and CDD but positively correlated with other extreme precipitation indexes. The AO index was negatively correlated with CDD and positively correlated with other extreme precipitation indexes. The correlation between SCSSMI and SAMSMI and the extreme precipitation index was the opposite to that of AO and the extreme precipitation index.

Conclusions

An analysis of changes in the trends of the extreme precipitation and temperature indexes in the Qilian Mountain area from 1971 to 2016 showed a larger warming range for the night index than the day index. In addition, the warming index of extreme temperature showed an increasing trend compared to the cold index. However, interannual changes in the warming index of extreme temperature were similar to those of the cold index of extreme temperature. The cold indexes (ID and FD) and warming indexes (TXX, TNX, and GSL) in the Qilian Mountains were larger than those in other areas, and there were fewer extremely low-temperature events in the Qilian Mountains compared to other areas, although there were more extreme high-temperature events. The climate warming trend in the Qilian Mountains was more obvious than that in other areas. The largest increases in the interannual variations of the PRCPTOT, RX5DAY, and R95 indexes in the Qilian Mountain area occurred in the 1980s and from 2000 to 2017, but the smallest increases (and even decreases) were noted in the 1990s. The change rates of rainy days, CWD, R10MM, R20MM, and R25MM were 5.79 d/10 a, 0.06 d/10 a, 0.40 d/10 a, 0.09 d/10 a, and 0.05 d/10 a, respectively. All of the daily indexes of extreme precipitation (except CWD) passed the significance level test of 5%. The percentage increases in rainy days, CWD, R10MM, R20MM, and R25MM, were 43.5%, 12.6%, 47.0%, 62.9%, and 64.6%, respectively. All of the daily indexes of extreme precipitation (except for CDD) showed increasing trends in the Hexi Inland River Basin, Qaidam Inland River Basin, and the Yellow River Basin. However, the increasing extents of CWD, R10MM, R20MM, and R25MM in the Yellow River Basin were lower than those in the Qilian Mountains. The warming ranges of the four indexes (TX10, TN10,

TXN, and TNN) decreased from south to north, but the spatial distributions of PRCPTOT, SDII, RX1DAY, RX5DAY, R95, and R99 were similar throughout the Qilian Mountain area. The largest region of increase was the central part of the Qilian Mountain area, but the region decreased from inside to outside. TX10, TN10, ID, and FD showed significant negative correlations with altitude, whereas TXN and TNN showed significant positive correlations with altitude. The most obvious changes in TX10, TN10, TXN, TNN, ID, FD, and DTR were seen in high-altitude areas (> 2500 m), and the most obvious changes in TN90, TX90, TXX, TNX, and GSL were seen in low altitude areas (< 2500 m). The Qilian Mountains, the Hexi Inland River Basin, and the Qaidam Inland River Basin were greatly affected by the AMO, NTA, CAR, SCSSMI, and SAMSMI, and they were slightly affected by the Nino4, NAO, NP, SOI, AO, and MEI. The index of extreme precipitation days in the Yellow River Basin was highly correlated with AO and SCSSMI. The effects of the circulation indexes (AMO, the TNA Index, the TSA Index, the North Tropical Atlantic SST Index, and the Caribbean SST index) on the extreme temperature warm index were stronger than those of the extreme cold temperature index. Furthermore, the Central Tropical Pacific SST was found to mainly affect the extreme cold temperature indexes, whereas the SCSSMI mainly affected the extreme warm temperature indexes.

References

Aguilar E, Aziz Barry A, Brunet M, Ekang L, Fernandes A, Massoukina M, ThambaUmba O (2009) Changes in temperature and precipitation extremes in western central Africa, Guinea Conakry, and Zimbabwe, 1955–2006. J Geophys Res Atmos 114(D2):1–11

Alexander LV, Zhang X, Peterson TC, Caesar J, Gleason B, Klein Tank AMG, Tagipour A (2006) Global observed changes in daily climate extremes of temperature and precipitation. J Geophys Res Atmos 111(D5):1042–1063

Almazroui M, Saeed S (2020) Contribution of extreme daily precipitation to total rainfall over the Arabian Peninsula. Atmos Res 231:1–8

Caesar J, Alexander LV, Trewin B, Tse-Ring K, Sorany L, Vuniyayawa V, Jayasinghearachchi DA (2011) Changes in temperature and precipitation extremes over the Indo-Pacific region from 1971 to 2005. Int J Climatol 31(6):791–801

Chen H, Fan S, Zhang X (2009) Seasonal differences of variation characteristics of extreme precipitation events over China in the last 50 years. Trans Atmos Sci 32(6):744–751

Cheng G, Wu T (2007) Responses of permafrost to climate change and their environmental significance, qinghai-tibet plateau. J Geophys Res Earth Surf 112(F2):1–10

Cheng Q, Gao L, Zuo X, Zhong F (2019) Statistical analyses of spatial and temporal variabilities in total, daytime, and nighttime precipitation indexes and of extreme dry/wet association with large-scale circulations of Southwest China, 1961–2016. Atmos Res 219:166–182

Choi G, Collins D, Ren G, Trewin B, Baldi M, Fukuda Y, Lias N (2009) Changes in means and extreme events of temperature and precipitation in the Asia-Pacific Network region, 1955–2007. Int J Climatol J R Meteor Soc 29(13):1906–1925

CMA Climate Change Centre (2021) Blue book on climate change in China (2021). Science Press, Beijing

Delworth TL, Mann ME (2000) Observed and simulated multidecadal variability in the Northern Hemisphere. Clim Dyn 16(9):661–676

Ding Z, Ge Y, GJilili A (2018) Trends of extreme temperature and precipitation in Ebinur Lake basin in Xinjiang during the period from 1957 to 2012. J Univ Chin Acad Sci 35(2):160–171 (**(In Chinese)**)

Du J, Lu HY, Jian J (2013) Variations of extreme air temperature events over Tibet from 1961 to 2010. Acta Ecol Sin 68:1269–1280

Du J, Lu HY, Yuan L (2016) Spatio-temporal change of extreme temperature events in Mt. Qomolangma Region of Tibet from 1971 to 2012. Arid Zone Res 33(1):20–27

Easterling DR, Evans JL, Groisman PY, Karl TR, Kunkel KE, Ambenje P (2000) Observed variability and trends in extreme climate events: a brief review. B Am Meteorol Soc 81(3):417–426

Folland CK, Palmer TN, Parker DE (1986) Sahel rainfall and worldwide sea temperatures, 1901–85. Nature 320(6063):602–607

Folland CK, Karl TR, Christy JR (2001) Observed climate variability and change [G] Climate Change 2001: The Scientific Basis, edited by J. H. Houghton et al. Cambridge University Press, New York, pp 99–181

Gao Y, Feng Q, Li ZX (2014) The variation of climate extremes in the Taolaihe River Basin in the Qilian Mountain area of China during 1957–2012. J Desert Res 34(3):814–826 (**(In Chinese)**)

He BR, Zhai PM (2018) Changes in persistent and non-persistent extreme precipitation in China from 1961 to 2016. Ad Clim Chang Res 9(3):177–184

IPCC (2013) Summary for policymakers. In: Climate Change 2013: the physical science basis. Contribution of Working Group I to the Fifth Assessment Report of the Intergovernmental Panel on Climate Change [Stocker, T.F., D. Qin, G.-K. Plattner, M. Tignor, S.K. Allen, J. Boschung, A. Nauels, Y. Xia, V. Bex and P.M. Midgley (eds.)]. Cambridge University Press, Cambridge

IPCC (2014) Summary for policymakers. In: Climate Change 2014: Impacts, Adaptation, and Vulnerability. Part A: Global and Sectoral Aspects. Contribution of Working Group II to the Fifth Assessment Report of theIntergovernmental Panel on Climate Change [Field, C.B., V.R. Barros, D.J. Dokken, K.J. Mach, M.D. Mastrandrea,T.E. Bilir, M. Chatterjee, K.L. Ebi, Y.O. Estrada, R.C. Genova, B. Girma, E.S. Kissel, A.N. Levy, S. MacCracken,P.R. Mastrandrea, and L.L. White (eds.)]. Cambridge University Press, Cambridge, pp. 1–32

Jing YH, Shen HF, Li XH, Guan XB (2019) A two-stage fusion framework to generate a spatio–temporally continuous modis ndsi product over the tibetan plateau. Remote Sen 11(19):1–21

Kunkel KE, Easterling DR, Redmond K, Hubbard K (2003) Temporal variations of extreme precipitation events in the United States: 1895–2000. Geophys Res Lett 30(17):1–5

Li Z, He Y, Theakstone WH, Wang X, Zhang W, Cao W, Chang L (2012) Altitude dependency of trends of daily climate extremes in southwestern China, 1961–2008. J Geograph Sci 22(3):416–430

Li ZX, Qi F, Wang QJ, Song Y, Li HY (2016) The influence from the shrinking cryosphere and strengthening evopotranspiration on hydrologic process in a cold basin, Qilian Mountains. Glob Planet Chang 144:119–128

Li L, Yao N, Li Y, Li Liu D, Wang B, Ayantobo OO (2019) Future projections of extreme temperature events in different sub-regions of China. Atmos Res 217:150–164

Lin P, He Z, Du J, Chen L, Zhu X, Li J (2017) Recent changes in daily climate extremes in an arid mountain region, a case study in northwestern China's Qilian Mountain area. Sci Rep 7(1):1–15

Meredith M, Sommerkorn M, Cassotta S (2019) IPCC special report on the ocean and cryosphere in a changing climate. Cambridge University Press, Cambridge

Pan ZT (2004) Altered hydrologic feedback in a warming climate introduces a "warming hole." Geophys Res Lett 31(17):L17109

Peterson TC, Folland C, Gruza G, Hogg W, Mokssit A, Plummer N (2001) Report of the Activities of the Working Group on Climate Change Detection and Related Rapporteurs, Tech. Doc. 1071, 146 pp., World Meteorol Organ, Geneva, Switzerland

Rashid IU, Almazroui M, Saeed S, Atif RM (2020) Analysis of extreme summer temperatures in Saudi Arabia and the association with large-scale atmospheric circulation. Atmos Res 231:1–12

Roy SS (2019) Spatial patterns of trends in seasonal extreme temperatures in India during 1980–2010. Weath Clim Extrem 24:1–7

Sangkharat K, Mahmood MA, Thornes JE, Fisher PA, Pope FD (2020) Impact of extreme temperatures on ambulance dispatches in London, UK. Environ Res 182:1–11

Singh N, Mhawish A, Ghosh S, Banerjee T, Mall RK (2019) Attributing mortality from temperature extremes: a time series analysis in Varanasi, India. Sci Total Environ 665:453–464

Stocker T F, Qin D, Plattner G K, Tignor M, Allen S K, & Boschung J (2014). Climate Change 2013: The Physical Science Basis. Contribution of Working Group I to the Fifth Assessment Report of IPCC the Intergovernmental Panel on Climate Change. AGU Fall Meeting Abstracts

Sui CJ, Zhang ZH, Yu LJ (2017) Investigation of Arctic air temperature extremes at north of 60°N in winter. Acta Oceanol Sin 36:51–60

Wei FY (1999) Modern climatic statistical diagnosis and forecasting technology. China Meteorological Press, Beijing (**(In Chinese)**)

Yin Y, Han C, Yang G, Huang Y, Liu M, Wang X (2020) Changes in the summer extreme precipitation in the Jianghuai plum rain area and their relationship with the intensity anomalies of the south Asian high. Atmos Res 236:104793

You Q, Kang S, Aguilar E, Pepin N, Flügel WA, Yan Y, Huang J (2011) Changes in daily climate extremes in China and their connection to the large scale atmospheric circulation during 1961–2003. Clim Dynam 36(11–12):2399–2417

Yu XL, Ren XS (1999) Multivariate statistical analysis. China Statistics Press (In Chinese)

Zhai P, Zhang X, Wan H, Pan X (2005) Trends in total precipitation and frequency of daily precipitation extremes over China. J Clim 18(7):1096–1108

Zhai PM, Pan XH (2003) Change in Extreme Temperature and Precipitation over Northern China During the Second Half of the 20th Century. Acta Geogra Sinica 1–10 (In Chinese)

Zhang PF (2020) Observed trend changes in extreme temperature over the global land, 1951–2018. China University of Geosciences, China (**(In Chinese)**)

Zhang J, Gou X, Pederson N, Zhang F, Niu H, Zhao S, Wang F (2018) Cambial phenology in Juniperus przewalskii along different altitudinal gradients in a cold and arid region. Tree Physiol 38(6):840–852

Zhao XY, Luo L, Wang YR (2014) Extreme temperature events in eastern edge of the qinghai-tibet plateau from 1963 to 2012. Resour Sci 36(10):2113–2122 (**(In Chinese)**)

Zhao RF, Su L, Zhu W (2017) Extreme temperature events in arid region of northwest china during 1961–2012: seasonal spatio-temporal analysis. Chin Agric Sci B 33(12):63–73 (**(In Chinese)**)

Zhao P, Gao L, Wei J, Ma M, Deng H, Gao J, Chen X (2020). Evaluation of ERA-Interim Air Temperature Data over the Qilian Mountains of China. Advances in Meteorology, 2020.

Zhou YQ, Ren GY (2010) Variation characteristics of extreme temperature indexes in mainland China during 1956–2008. Clim Environ Res 15(4):405–417

Zhou Y, Ren G (2011) Change in extreme temperature event frequency over mainland China, 1961–2008. Clim Res 50(2–3):125–139